https://doi.org/10.46389/rjd-2024-0418
www.jrdiabet.ro

Rom J Diabetes Nutr Metab Dis
2024; Volume 31, Issue 1, pages 418-432

MANAGING THE IMMUNE MARKERS TO RHEUMATOID ARTHRITIS WITH CHITOSAN-CAPPED GOLD NANOPARTICLES

Marwa Dawood Jaaffer[1]*, Israa Ali Zaidan Al-Ogaidi
Department of Biotechnology, College of Science, University of Baghdad, Bagdad, Iraq

Abstract

Gold nanoparticles (AuNPs) were functionalized by coating with chitosan (CS) and utilized to manage the immune response of 84 rheumatoid arthritis patients and 20 healthy volunteers ranging in age from 18 to 80 years. The synthesized gold nanoparticles, before and after functionalization, were characterized by UV-Vis spectrophotometer, Fourier-transforms spectroscopy, X-ray diffraction, zeta potential, and FE-SEM. The results of the FE-SEM analysis revealed that the AuNPs, both before and after functionalization, with chitosan, were spherical in shape, while they had size range of 20–50 and 40- 117 nm, respectively. Zeta potential analysis revealed that the NPs had a negative (-34 mV) and positive surface charge (+64 mV) before and after functionalization, respectively. The levels of 10 immune markers in the sera of RA patients (IgA, IgE, IgG, RF, ANA, anti-dsDNA, C3, C4, IL-6, and IL-33) were tested by ELISA kits to study the *in vitro* effects of treatment with functionalized and non-functionalized AuNPs on their immune response. The levels of all markers were decreased significantly in RA patients after exposure to AuNPs or AuNPs-CS. However, the levels of IgA, IgE, IgG, ANA, anti-dsDNA, C3, C4, and IL-6 showed significantly higher reduction in the presence of AuNPs as compared to AuNPs-CS, whereas the opposite was observed for the levels of RF and IL-33.

Keyword: Nanotechnology, gold nanoparticles (AuNPs), chitosan (CS), Rheumatoid arthritis (RA), ELISA.

Introduction

Rheumatoid arthritis (RA) is a chronic autoimmune systemic disease that primarily damages the lining of synovial joints. It causes progressive disability, premature death, and has a significant economic impact [1]. It is critical to understand how pathologic mechanisms lead to the deterioration of RA progression in individuals in order to design medicines that effectively treat patients at each stage of their disease [2]. Pharmacologic therapy (including conventional, biological, and innovative molecular disease-modifying anti-rheumatic medicines) has achieved remarkable progress toward disease recovery without joint deformity. Nonetheless, a considerable proportion of RA patients do not react successfully to existing medications [3]. The available medication specifically targets macrophage proliferation and the production of pro-inflammatory cytokines. The therapeutic effectiveness of current treatment options at the targeted site is limited. Therefore, there is a pressing need to develop a new therapeutic method that could give more targeted drug delivery and make it safer.

* Email: Marwa.Jaafer1106@sc.uobaghdad.edu.iq

Chitosan (CS) is a natural polysaccharide generated from biodegraded, bio compliant, non-toxic chitin that has antifungal, anticancer, and antibacterial properties [4,5]. It can be employed as a stabilizer to alter nano composite properties and to provide nanoparticles with long-term stability by preventing particle aggregation [6]. The only natural cationic polysaccharide is chitosan. Finally, whether these pro-inflammatory or anti-inflammatory responses are beneficial or detrimental depends on the situation [7]. Nanotechnology is becoming increasingly essential in modern research. Nanotechnology is focused on the formation and implementation of nanomaterials, also defined as materials with dimensions less than 100 nm [8], which are referred to as nanomaterials. Nanomaterials perform well in a number of applications because they have a higher surface-to-volume ratio [9].

Gold compounds have been used to treat RA for more than 50 years, dating back to Jacques Forestier's [10] discoveries in the early 1930s. AuNPs have lately been employed as drug delivery vehicles for molecules such as DNA, peptides, anticancer medicines, and antibody products [11]. It is known that the properties vary according to the size, shape, medium, cell type, charge, and nanoparticle synthesis reduction agent [12]. It is important to study the effects of AuNPs on their own before putting them together with other drugs. This will help find the best way to use them in therapy.

Previously, some studies used nanoparticles to control RA disease, such as that of Li et al. who used the nano-conjugates GNPs/MTX-Cys-FA to decrease the expression and secretion of inflammatory factors. They found that the GNPs/MTX-Cys-FA can drastically reduce rheumatoid synovitis and successfully protect articular cartilage [13]. Moreover, Cui et al. proposed treating RA using highly bioavailable embelin-loaded chitosan nanoparticles (CS-embelin NPs). Their findings revealed that the CS-embelin NPs had antioxidant and anti-inflammatory impacts which protected rats against adjuvant-induced arthritis [14].

Therefore, research based on nanomaterial has a reflective impact within medical science. The development of therapeutic inorganic nanoparticles is a crucial aspect of nanomedicine. The importance of NPs in medicine and biology has risen dramatically in recent years. However, nothing is known regarding their impact on rheumatic diseases treatment [15].

Materials and methods

Materials

Chloroauric acid trihydrate (HAuCl4·3H2O), trisodium citrate dehydrate Na3C6H5O7·2H2O (99.0%), trypsin-EDTA, fetal bovine serum, 3-(4,5-dimethylthiazal-z-yl)-2,5-diphenylterazolium (MTT), and crystal violate stain were purchased from Sigma Chemical Co. (St. Louis, MO, USA). RPMI-1640 medium was purchased from Gibco (USA), chitosan from Bio-World US, and the kits from CUBSBIO.

Patients and serum samples

This study included the collection of residual sera from 84 patients and 20 healthy volunteers from Baghdad's Dowaly Private Hospital and Medical City/Educational Laboratories

during the period from June to September 2021. Patients' blood samples were taken in tubes. Serum was taken out of blood by centrifuging and kept in small amounts at -18 °C until time of test.

Ethical Consideration

The Baghdad University Ethics Board approved the study. The Declaration of Helsinki, the code of ethics of the World Medical Association, was followed when conducting this research on humans

Preparation of gold nanoparticle

Synthesis of AuNPs was carried out using the following procedure of Turkevich et al. (1951); a volume of 100 mL of 1 mgml $^{-1}$ trisodium citrate solution was heated to 100°C to make AuNPs with a nanoscale diameter of 20 nm [16]. Following that, 2 mL of 5mgml^{-1} HAuCl4.H2O solution was promptly added to the trisodium citrate solution while vigorously stirring at 100 °C. After 10 minutes, the solution's color changed to red wine, followed by the formation of AuNPs. The solution was then allowed to cool down to room temperature while being constantly stirred.

Preparation of chitosan-capped gold nanoparticles

AuNPs-CS were prepared using 10 mL of AuNPs, which were initially stirred at room temperature. Then, 1.5 mL of 0.0025 mgml^{-1} chitosan solution (made by dissolving 0.25% chitosan powder in 100 mL of D.W in 1% acetic acid) was added, then heated for 15 minutes and stirred for 15 minutes at room temperature to achieve chitosan capped AuNPs).

Characterization of AuNPs and AuNPs-CS

The reduction of AuNPs and AuNPs-CS ions was analyzed by using U-2910 spectrophotometer (Hitachi, Japan). Continuous scanning at a wavelength of 200–600 nm was used to perform UV–vis spectroscopic analysis. The AuNPs and AuNPs-CS solutions were next examined using an X-ray diffractometer (XRD-6000, Shimadzu, Japan). A Cu K incident beam (= 1.542 A°) at 2θ = 20°–60° was used to generate the diffraction pattern. The X-ray tubes' voltage and current were 40 kV and 30 mA, respectively. The size was determined using the Debye-Scherrer equation, $D = 0.94\ \lambda / \beta \cos \theta$. The FTIR study was performed using an FTIR spectrometer (8400S, Shimadzu, Japan) in attenuated total reflection mode with a spectrum range of 4000–400 cm^{-1} and a resolution of 4 cm^{-1}. Finally, additional examinations were performed by employing an FE-SEM device (Shimadzu AA-7000, Japan).

Serological parameters

Indirect ELISA protocol

Standard serial diluted solutions were prepared for the immunoglobulins IgA (1000, 250, 62.5, 15.6, 3.9, 0.89, 0.24, 0 ng/ml), IgE (0,50, 150, 373, and 1250 ng/ml), and IgG (100, 50, 25, 12.5, 6.25, 3.13, 1.56, and 0 ng/ml). After dispensing 100 µl of samples and standards into pre-assigned wells, the plate was incubated for 2 hours at 37°C, and each well was washed three times

with 200 µl of wash buffer per well. After washing, 100 µl of AuNPs and AuNPs-CS were dispensed in each well, and the plate was incubated for 120 minutes at 37 °C before being washed twice. After washing, in each well, 100 µl of HRP-conjugate was added, and the plate was incubated at 37 °C for 60 minutes. After washing, TMB substrate (90 µl) was spread in each well, and blue colors of varying densities developed in the wells within 15–30 minutes. A volume of 50 µl of stop solution was then added to stop the reaction., causing the wells to turn yellow. Finally, the absorbance was read at 405 nm.

Sandwich ELISA protocol

Standard serial diluted solutions were made for the complement compounds C3 (300, 150, 75, 37.5, 18.75, 9.4, 4.7, and 0 ng/ml) and 4 (300, 100, 33.3, 11.1, 3.7, 1.23, 0.41, and 0 ng/ml), as well as the interleukins IL-6 (500, 250, 125, 62.5, 31.2, 15.6, 7.8, and 0 ng/ml) and IL-33 (1000, 500, 250, 125, 62.5, 31.2, 15.6, and 0 ng/ml). A volume of 100 µl of samples and standards was transferred into pre-assigned wells and the plate was incubated for 2 hours at 37°C. After incubation, the contents of the wells were removed, and each well was washed twice with 200 µl of wash buffer per well. Following washing, 100 µl of AuNPs and AuNPs-CS were dispensed into each well, and the plate was incubated at 37 °C for 120 minutes before being washed twice. After washing, in each well, 100 µl of HRP-conjugate was added, and the plate was incubated at 37 °C for 60 minutes. After washing, TMB substrate (90 µl) was spread in each well, and blue colors of varying densities developed in the wells within 15–30 minutes. A volume of 50 µl of stop solution was then added to stop the reaction., causing the wells to turn yellow. Finally, the absorbance was read at 405 nm.

Statistical analysis

The data was coded, processed, and analyzed using the Statistical Package for Social Sciences (SPSS) version 22 for Windows (IBM SPSS Inc, Chicago, IL, USA). Quantitative information was presented as mean SD (Standard deviation), independent groups of normally distributed variables were compared using the one-way ANOVA. P value < 0.05 was regarded as significant.

Results and discussion

Preparation of gold nanoparticles: Turkevich proposed in 1951 that tetrachloroauric acid may be reduced by trisodium citrate at high temperatures to produce gold nanoparticles with a size of roughly 20 nm (Turkevich et al., 1951). The process resulted in a progressive shift in coloring that progressed from pale yellow to bluish grey, purple, and finally red, indicating the creation of AuNPs [16]. A model of the citrate method has been designed for producing for producing gold nanoparticles. It suggests that the oxidation of trisodium citrate to dicarboxy acetone converts Au^{3+} to Au^{+}. At the experiment-related temperatures, dicarboxy acetone decomposes. The disproportionation of Au+, which is also accelerated by the gold surface, produces gold atoms, and it is this reaction that results in the development of nuclei as well as growth.The development of a multimolecular complex between dicarboxy acetone and AuCl is necessary for nucleation; as a result, the rate of nucleation is significantly impacted by dicarboxy acetone degradation.

The second step involved the fabrication and functionalization of the prepared AuNPs with chitosan. Chitosan can operate as an electrostatic stabilizer, offering a twofold benefit by

delivering an appropriate charge through the amino groups, which will aid in the following attachment of biomolecules. When used in conjunction with AuNPs, chitosan acts as a stabilizing agent. It prevents particle aggregation [17].

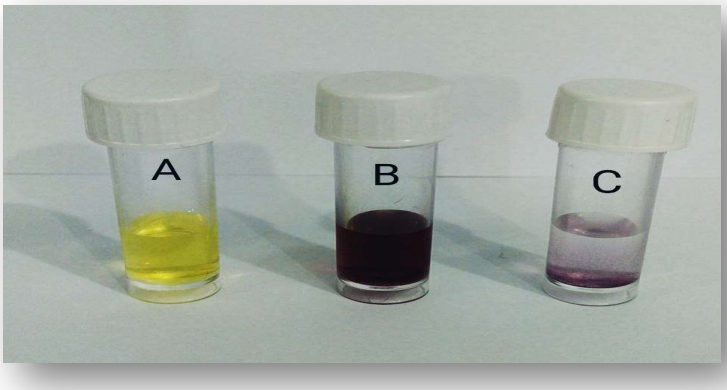

Figure 1- Gold nanoparticles (AuNPs) preparation. (A) Suspensions of gold salt solution ($HAuC_{l4}.3H_2O$). (B) Gold nanoparticles (AuNPs). (C) Functionalization of AuNPs with chitosan (AuNPs-CS).

Characterization of AuNPs and AuNPs–CS

UV-Vis Spectrophotometry

The UV–vis absorption spectra of gold nanoparticles are depicted in Figure 2. The higher absorption at 528 nm revealed that AuNPs were successfully synthesized, which is consistent with the findings of Al-Dulimi et al., 2020 who reported that the absorbance peak of gold nanoparticles was at 522 nm [18]. At regular intervals, the synthesis of CS-AuNPs was monitored using a UV spectrophotometer. Figure 2 (red line) shows a shift in the surface Plasmon resonance band (SPRB) in the UV spectrum from 528 nm to 535.5 nm, which indicated the formation of AuNPs-CS. In a similar way, Saravanakumar et al.,2020 found the SPRB in the range of 520 nm to 560 nm, which showed that AuNPs-CS were probably made [19].

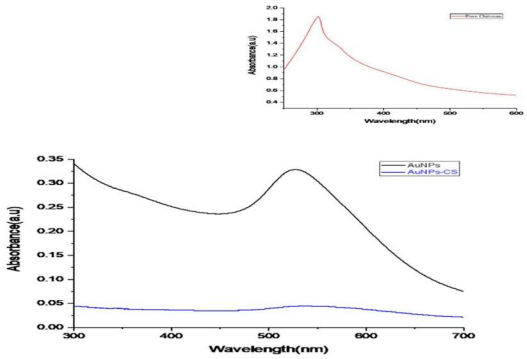

Figure 2- UV–vis absorption spectra of AuNPs and AuNPs-CS. Experiments performed at room

temperature.

Fourier transform infrared spectroscopy analysis

The chemical surfaces and functional group endpoints of AuNPs and AuNPs-CS were characterized using FT-IR spectroscopy (Figure 3). The spectra showed an average of 20 scans that were seen between 4000 and 500 cm^{-1}. The peak at 3255cm^{-1} reflected an OH functional group as well as a medium-strength H-bounded vibration. Furthermore, a detected peak at 2117.84cm^{-1} and 1631.78 cm^{-1} was belonged to the symmetric and anti-symmetric stretching of C=O and the 1531 cm^{-1} signal was attributed to gem-dimethyl, "iso" phenol, or a tertiary O-H group. It was found that many aromatic (C=C) bonds have medium stretch vibrations at peaks between 1400 and 1200 cm^{-1}. In the current investigation, the FTIR spectra of chitosan capped gold nanoparticles showed essentially identical peaks to those of pure chitosan, demonstrating homogeneous chitosan deposition over gold nanoparticles. The sole difference between AuNPs and AuNPs-CS in the FTIR is the shift of a broad band between 3255.84 cm^{-1} to 3259.70 and 1631.78 to 1641.23 cm^{-1} and the removal of a peak at 2850 cm^{-1}.

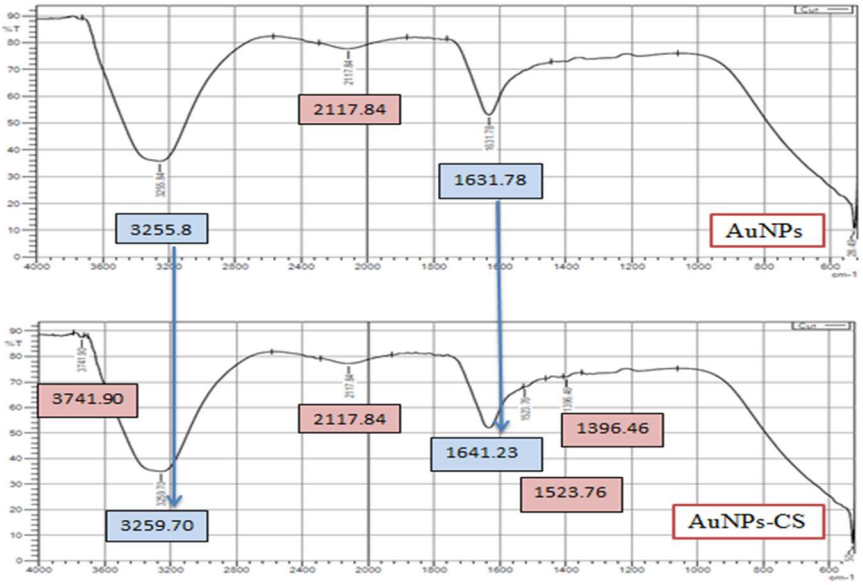

Figure 3- FT-IR analysis of AuNPs and AuNPs-CS

X-Ray diffraction analysis

The crystalline phase of AuNPs, CS, and AuNPs-CS was investigated using XRDThe results of the XRD structural examination of AuNPs, CS, and AuNPs-CS are shown in Figure4. The Bragg's reflections of (111), (200), (220), and (311) planes, associated to the face-centered cubic (FCC) of AuNPs, are correlated with the strong diffraction peaks with 2θ values at 38.2º, 44.4º, 64.7º, and 77.7º. The diffraction peaks found were identical to those published for standard gold metal (Au^0) (Joint Committee on Powder Diffraction Standards JCPDS no. 04-0784, USA). The XRD pattern revealed that AuNPs and AuNPs-CS were significantly crystalline. Also, it was

found that the AuNPs had all of the AuNPs-CS diffraction peaks. This shows that the structure of the AuNPs is stable in the presence of CS. Scherrer's formula was used to calculate the crystalline size of Au nanoparticles, as follows:

$$D = 0.89\lambda/\beta \cos \theta$$

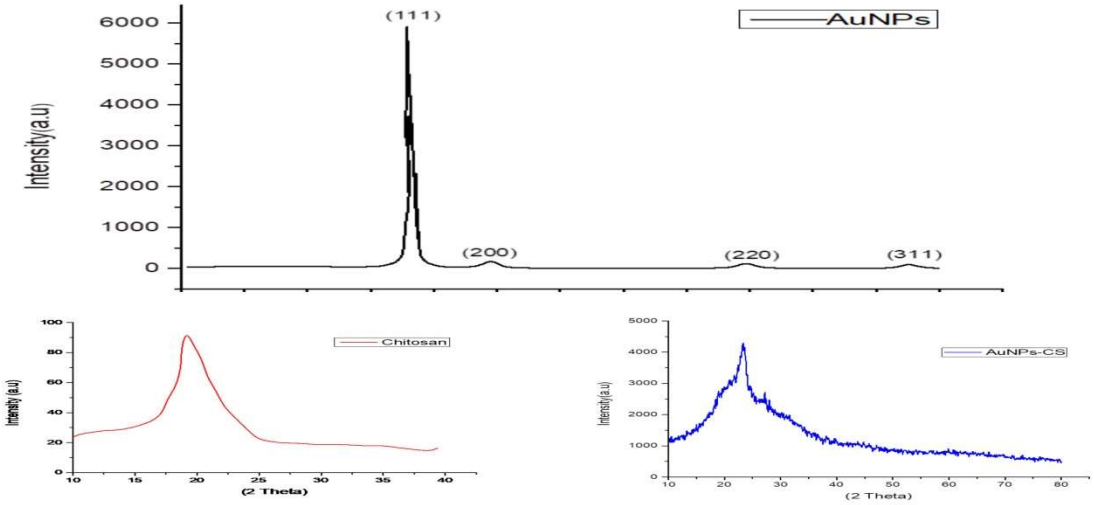

Figure 4- The XRD patterns of AuNPs, Chitosan, and AuNPs-CS.

Field Emission Scanning Electron Microscopy

The FE-SEM image revealed more about the morphology and size of the nanoparticles. The AuNPs showed smooth, well-separated structures, spherical form, and a size range of 20–50 nm nm, as illustrated in Figure 5, with appropriate size distribution. Almost all of the particles had a single distribution with clear homogeneity and no aggregations (Figure 5: right lane). This might be the result of AuNP's citrate reduction in a polar solvent. Citrate ions can give the surface of AuNPs a negative charge, which makes it easy for them to spread out [19]. The surface morphology of the AuNPs-CS was studied using FE-SEM device, as shown in Figure 5: left lane. The crystals have a spherical shape with a size range of 40 to 117 nm.

The Zeta Potential Analysis

Analysis of particle size and zeta potential were carried out to better characterize AuNPs and AuNPs-CS, using a zeta size machine. AuNPs have an average size of 40 nm (Figure 6: upper side). The zeta potential of NPs varies depending on their surface chemistry. Due to the presence of citrate molecules at their surface, which were used as a reducing agent during the production process, uncoated AuNPs possessed a negative surface charge (-34 mV). The charge on AuNPs-CS was positive (+64) (Figure 6: lower side).

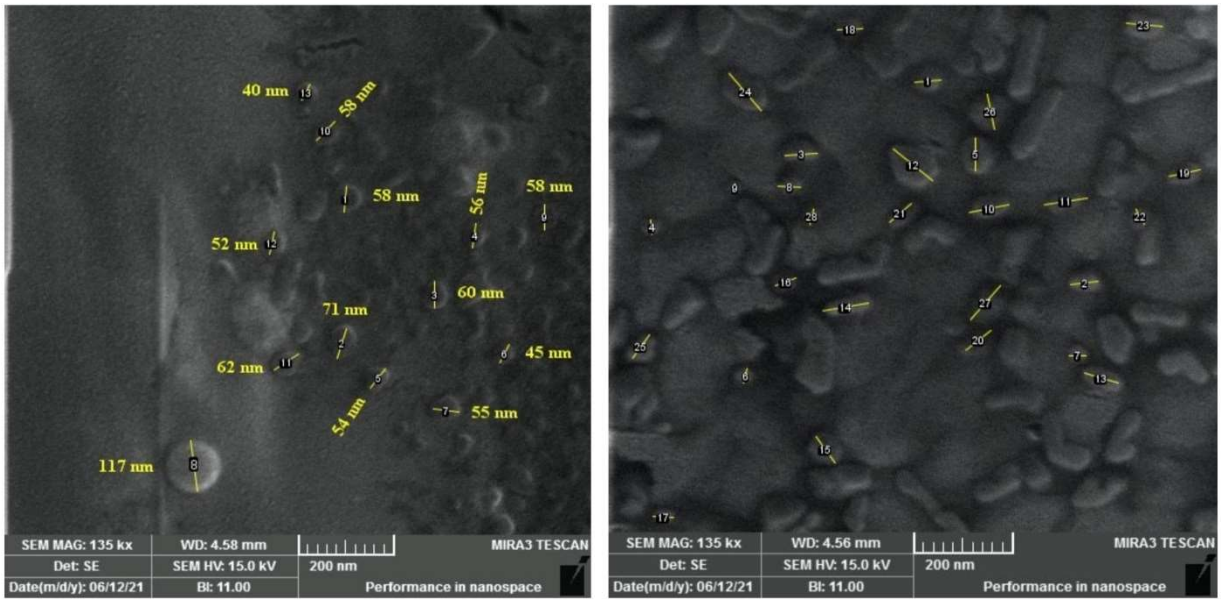

Figure 5- FE- SEM image of AuNPs (right lane) and FE- SEM image of AuNPs-CS (left lane) showing spherical and uniformly distributed nanoparticles.

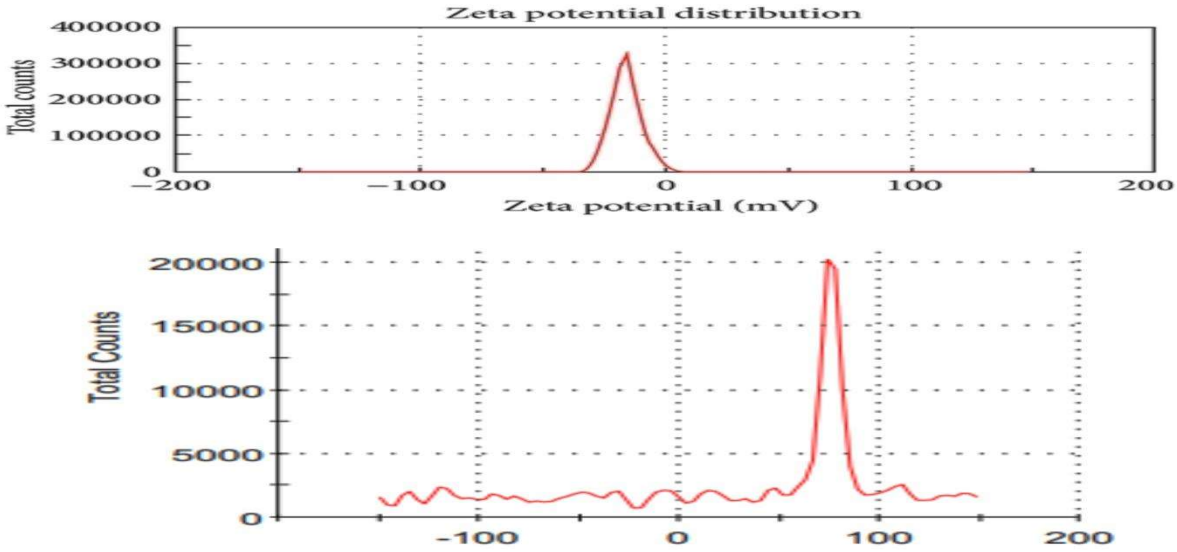

Figure 6- Zeta potential analysis for AuNPs and AuNPs-CS.

Effects of AuNPs and AuNPs-CS on serological parameters

Table 1 displays the ELISA kit results for immune markers (immunoglobulins (IgA, IgE, IgG), autoantibodies (rheumatoid factor (RF), antinuclear antibodies (ANA), anti-double stranded DNA (Anti-dsDNA)), complement compounds (C3, C4), and interleukins (IL-6, and IL-33)). There was a significant reduction in the values of all these parameters in the serum samples of RA patients ($P< 0.001$) when compared to the values of the healthy individuals group.

Immune markers	Healthy people (n=20)	rheumatoid arthritis (n=20)	Control (before exposing NPs)	Exposing AuNPs (n=28)	exposing AuNPs-CS (28)

		P <0.001	**(n=28)**	P <0.001	P <0.001
			Immunoglobulin		
IgA	89.44± 52.17	277.97± 89.54	207.74±58.696	52.73±44.178,	54.45±31.856
IgE	15.39± 13.46	64.25 ± 42.81	76.45±36.401	3.77±0.943,	5.06±2.720
IgG	9.57± 2.64	189.65±101.74	153.12±57.24	16.94±23.25	23.50±23.91
			Autoantibodies		
RF	114.11± 13.57	160.40± 29.87	166.12±22.88	91.64±14.14	92.49±14.31
ANA	0.20±0.05	0.68±0.20	0.65±0.17	0.13±0.1	0.15±0.0
Anti-dsDNA	0.20±0.02	0.54±0.22	0.58±0.15	0.16±0.08	0.16±0.1
			Complement compounds		
C3	71.96±32.76	122.84 ±48.66	156.09±0.15	32.53±9.06	49.66±25.46
C4	35.80±16.20	58.03±23.35	71.19±22.79	16.43±5.28	28.76±12.26
			Interleukins		
IL-6	22.89± 12.59	41.15± 8.28	39.60±8.07	12.33±3.57	14.51±6.09
IL-33	77.96± 52.31	252.69±120.54,	271.76±62.97	70.20±78.08	34.23±50.42

Table 1- The serum levels of immune markers (IgA, IgE, IgG, RF, ANA, Anti-dsDNA, C3, C4, IL-6 and IL-33) in rheumatoid arthritis (RA) patients and healthy people. These immune markers were measured by ELISA kit in sera of RA patients before and after exposing the samples to AuNPs and AuNPs-CS.

Next, all the 10 immune markers were evaluated to compare their levels in the serum samples of RA patients before and after AuNPs and AuNPs-CS exposure. The levels of all markers dropped rapidly in RA patients following exposure to AuNPs and AuNPs-CS, as compared to the control group (before exposure). The reduction was highly significant (P<0.001) and serum levels of these markers were recovered to normality in the groups exposed to both types of nanoparticles (AuNPs and AuNPs-CS).

The levels of 8 markers, namely IgA, IgE, IgG, ANA, Anti-dsDNA, C3, C4, and IL-6, were lower after AuNPs exposure than after AuNPs-CS exposure. Gold compounds have been characterized as having an immunosuppressive impact by decreasing the production of pro-inflammatory cytokines such as TNF-, IL-6, and IL-1 [21]. Poly lactic-co-glycolic acid(PLGA)nanoparticles actively transport therapeutic payloads to RA joints while blocking inflammatory cytokines. The high accumulation and lengthy retention of biomimetic nanocarriers in inflamed joints after intravenous injection resulted in good therapeutic effects [22]. The lower levels of these 8 immune markers after AuNPs exposure as compared to those after AuNPs-CS exposure can be also explained by particle size, which is known as an important factor. It was shown that cells are

more likely to import smaller NPs by endocytosis or diffusion, while bigger NPs were found to be more likely to be imported into cells via phagocytosis [23]. The amount of free energy generated by ligand–receptor interactions and the kinetics of receptor diffusion onto the wrapping sites on the cellular membrane are two parameters that determine how quickly and how many nanoparticles enter the cellular compartment via wrapping [24]. Huang et al.,2013 recently demonstrated that smaller NPs exhibit unique advantages over those larger than 10 nm in terms of their ability to interact with cells, which is most likely to blame for this result. The surface characteristics of smaller AuNPs were discovered to be different from those of the larger nanomaterials, and this is often reflected in changes in the frequency and intensity of the corresponding surface plasmon resonance peaks. [25]

However, the levels of the 2 other studied markers, namely RF and IL-33, were lower after AuNPs-CS exposure than after AuNPs exposure. Chitosan is polycationic, biodegradable, biocompatible, and mucoadhesive by nature, making it ideal for drug delivery [26]. Chitosan's biological applications are also enhanced by its ease of physical and chemical changes [27]. By varying the molecular weight and degree of deacetylation of chitosan, different physicomechanical characteristics can be achieved. Chitosan is a natural substance that is utilized extensively in pharmaceutical and biological applications. Researchers have explored chitosan nanoparticles extensively for their controlled drug release capabilities, and they have been used in both in vitro and in vivo applications [28]. Similar findings were also reported by Jhaveri et al. who revealed that chitosan nanoparticles can be actively used in the treatment of rheumatoid arthritis [29].

After being exposed to AuNPs and AuNPs-CS, IgA, IgE, IgG, RF, ANA, and dsDNA levels were reduced rapidly in RA patients. The exposure to these materials may be responsible for antibody destruction in different regions of their structure; one part of the antibody, the antigen-binding fragment (Fab), recognizes the antigen, whereas the other part, the crystallizable fragment (Fc), interacts with other immune system elements, such as phagocytes or complement pathway components, to promote antigen removal. There has been no prior research to our knowledge that has investigated the roles of nanoparticle in RA management. Oriented covalent binding may boost antibody stability and control the accessible protein binding sites by binding to the Fc region while leaving the antigen-binding site Fab region oriented to the medium in a ratio of one to one [30]. It is advantageous if the attachment of the antibody to the nanoparticle via its Fc region is relatively simple, without affecting antibody activity. This interaction is stable in high ionic concentration solutions and allows for a high antibody load per nanoparticle [30]. The direct attachment of the Fab to the surface of the nanoparticles is another option where a precise orientation of the antibody is not required [31]. Complement proteins and nanoparticles interact in a complex manner that is controlled by a variety of factors of interfacial dynamic forces and physicochemical variables [32]. Surface curvature and flaws are examples, as are functional groups and their surface density, as well as polymeric decorating and architectural displays. Some pathogens have developed and implemented complex surface and interfacial methods to avoid complement activation and death, as well as to disrupt complement-mediated opsonization processes [33]. It is important to understand these events for designing and making nanomedicines that are safe for the immune

system and can be used in the clinic. The study of Chen et al. found that when nanoparticles are intravenously injected into the mice body, complement proteins deposit on the surface of nanoparticles in a process called opsonization [34]. Kondo and Mihara (1995) focused less on the biological implications and more on the physical features of protein binding and their impacts on protein function. They established that high NP-protein affinities result in larger protein conformational alterations and, as a result, more irreversibility in adsorption and conformational states. This raises the question of whether a change in conformation can render a protein inactive or at the very least impede its function if it adsorbs to a nanoparticle. Finally, the interaction of proteins with nanoparticles may suppress or enhance protein function [35].

Reducing the generation of pro-inflammatory cytokines is the main goal of current RA treatment plans. Additional in vivo experiments on therapeutic effects revealed that the inhibition of pro-inflammatory cytokine release by the manufactured nanosystems has positive therapeutic effects on rats with AIA. Moredata points to the possibility that NPs can attach proteins to their surfaces [36,37]. These interactions have a variety of effects. It is possible that neither the protein function nor the particle characteristics and subsequent toxicity are impacted by the protein/particle interaction. Alternately, the particles' surface reactivity may cause them to alter or disrupt the protein's structure, which would reduce its functionality [38]. A different hypothesis is that protein binding changes the particle surface, lowering or changing its activity and the biological activity that results. Finally, the particles' large surface areas allowed them to bind a quantity of a particular protein.

Conclusions

Our study found that IgA, IgE, IgG, RF, ANA, Anti-dsDNA, C3, C4, IL-6, and IL-33 levels decreased rapidly in RA patients' sera after AuNPs and AuNPs-CS exposure and that the reduction was highly significant ($P < 0.001$) in comparison with the control.

Conflict of interest: Nil

Sources of finding: Nil

Author contribution: Nil

Acknowledgments

The authors are keen to thank everyone who participated in the study.

Reference

[1] M.M. Sampoorna, S. V. Bhavani, and B. K. Ponnakanti. Ortholord Tablets “Nutritional

Support for Rheumatoid Arthritis" *Mediterranean Journal of Basic and Applied Sciences (MJBAS)*, vol. 4, no. 2,pp 29-40, 2020, DOI: 10.46382/MJBAS.2020.4204
[2] Q.Guo, Y. Wang, D. Xu, J. Nossent N. J. Pavlos, and J. Xu, "Rheumatoid arthritis: pathological mechanisms and modern pharmacologic therapies". *Bone research*, vol. 6, no.1, pp 1-14, 2018, https://doi.org/10.1038/s41413-018-0016-9
[3] J. S. Smolen, R. Landewé, J. Bijlsma, G. Burmester, K. Chatzidionysiou, M. Dougados, and D.Van Der Heijde, "EULAR recommendations for the management of rheumatoid arthritis with synthetic and biological disease-modifying antirheumatic drugs: 2016 update". *Annals of the rheumatic diseases*, vol. 76, no.6, pp 960-977, 2017, . doi: 10.1136/ard.2009.126532
[4] R. Parhi. "Drug delivery applications of chitin and chitosan: a review". *Environmental Chemistry Letters*, vol.18, no.3, pp 577-594, 2020
[5] G. Sarwar, M.S. Hossain, M. Harun-Ur-Rashid and S. Parveen, "Assessment of genetic variability for agro-morphological important traits in aman rice (Oryza sativa L.)". *International Journal of Applied Sciences and Biotechnology*, vol.3, no. 1, pp73-79,2015, DOI: https://doi.org/10.3126/ijasbt.v3i1.11896
[6] Z. Chen, Z. Wang, X. Chen, H. Xu and J.Liu, "Chitosan-capped gold nanoparticles for selective and colorimetric sensing of heparin". *Journal of nanoparticle research*, vol. 15 no. 9, pp1-9, 2013, https://doi.org/10.1007/s11051-013-1930-9
[7] D. Fong and C.D. Hoemann, "Chitosan immunomodulatory properties: perspectives on the impact of structural properties and dosage". *Future science OA*, vol. 4, no.1, p FSO225, 2017, doi.org/10.4155/fsoa-2017-0064
[8] T. A. Saleh,Nanomaterials: "Classification, properties, and environmental toxicities". *Environmental Technology & Innovation*, no. 20, P 101067.,2020, doi.org/10.1016/j.eti.2020.101067
[9] N. Karak, "Fundamentals of nanomaterials and polymer nanocomposites". *In Nanomaterials and polymer nanocomposites,* pp. 1-45, 2019, doi.org/10.1016/B978-0-12-814615-6.00001-1
[10] K. Koushki, S. Keshavarz Shahbaz, M. Keshavarz, E.E. Bezsonov, T. Sathyapalan, and A. Sahebka, "Gold nanoparticles: Multifaceted roles in the management of autoimmune disorders". *Biomolecules*, vol. 11, no. 9, pp1289., 2021, doi.org/10.3390/biom11091289
[11] K. Bromma, K. and D.B. Chithrani, "Advances in gold nanoparticle-based combined cancer therapy". *Nanomaterials*, vol,10 no. 9, P1671, 2020, doi.org/10.3390/nano10091671
[12] M.S. Boyles, T. Kristl, A. Andosch, M. Zimmermann, N. Tran, E. Casals, and A. Duschl, "Chitosan functionalisation of gold nanoparticles encourages particle uptake and induces cytotoxicity and pro-inflammatory conditions in phagocytic cells, as well as enhancing particle interactions with serum components". *Journal of nanobiotechnology*, vol,13, no. 1, p 1-20,2015, doi.org/10.1186/s12951-015-0146-9
[13] X. Li, H. Wang, X. Zou, H. Su, and C. Li, "Methotrexate-loaded folic acid of solid-phase synthesis conjugated gold nanoparticles targeted treatment for rheumatoid arthritis". *European Journal of Pharmaceutical Sciences*, vol.170, p 106101, 2022, doi.org/10.1016/j.ejps.2021.106101

[14] P. Cui, F. Qu, N. Sreeharsha, S. Sharma, A. Mishra, and S.K. Gubbiyappa, "Antiarthritic effect of chitosan nanoparticle loaded with embelin against adjuvant-induced arthritis in Wistar rats". *IUBMB life*, vol,72, no. 5, pp 1054-1064,2020, doi.org/10.1002/iub.2248
[15] E. Nogueira, A.C. Gomes, A. Preto, and A. Cavaco-Paulo,.". *Nanomedicine: Nanotechnology, Biology and Medicine*, 2016, vol. 12, no. 4, pp 1113-1126., doi.org/10.1016/j.nano.2015.12.365
[16] J. Turkevich, P.C. Stevenson and J. Hillier, "A study of the nucleation and growth processes in the synthesis of colloidal gold". *Discuss. Faraday Soc*., vol,11, pp. 55-75, 1951, doi.org/10.1039/DF9511100055
[17] J.T. da Silva and A.S. Amaral, "Nanotechnology for Antifungal Therapy". *Nanobiotechnology in Diagnosis, Drug Delivery, and Treatment*, pp 259-271,2020, doi.org/10.1002/9781119671732.ch13

[18] A.G. Al-Dulimi, A. Z. Al-Saffar, G.M Sulaiman, K.A. Khalil, K. S., Khashan, H.S. Al-Shmgani, and E.M. Ahmed, "Immobilization of l-asparaginase on gold nanoparticles for novel drug delivery approach as anti-cancer agent against human breast carcinoma cells". *Journal of Materials Research and Technology*, vol, 9, no. 6, pp15394-15411,2020, doi.org/10.1016/j.jmrt.2020.10.021

[19] K. Saravanakumar, A.V.A Mariadoss, A. Sathiyaseelan, and M.H. Wang, "Synthesis and characterization of nano-chitosan capped gold nanoparticles with multifunctional bioactive properties". *International Journal of Biological Macromolecules*, vol.165, pp 747-757,2020, doi.org/10.1016/j.ijbiomac.2020.09.177
[20] L.C.Crowley, B.J. Marfell and N.J. Waterhouse, "Analyzing cell death by nuclear staining with Hoechst 33342". *Cold Spring Harbor Protocols*, no. 9, pdb. prot087205, 2016, doi:10.1101/pdb. prot087205
[21] J. Bondeson, "The mechanisms of action of disease-modifying antirheumatic drugs: A review with emphasis on macrophage signal transduction and the induction of proinflammatory cytokines". *General Pharmacology: The Vascular System*, Vol. 29, pp 127–150, 1997, doi.org/10.1016/S0306-3623(96)00419-3
[22] Q. Wang, X. Qin, J. Fang, and X. Sun, "Nanomedicines for the treatment of rheumatoid arthritis: State of art and potential therapeutic strategies". *Acta Pharmaceutica Sinica B*, vol,11 no. 5, pp1158-1174,2021, doi.org/10.1016/j.apsb.2021.03.013
[23] M. Wu, H. Guo, L. Liu, Y. Liu, and L. Xie, "Size-dependent cellular uptake and localization profiles of silver nanoparticles". *International journal of nanomedicine*, vol.14, P 4247, 2019, doi: 10.2147/IJN.S201107
[24] A.A. Rahman, A. A. Aziz, S. Shamsuddin, and A.R. Ibrahim, "The Effect of Gold Nanoparticle Size in the Cellular Uptake". *In Solid State Phenomena. Trans Tech Publications Ltd*. Vol. 290, pp. 75-80, 2019, doi.org/10.4028/www.scientific.net/SSP.290.75
[25] X. Huang, Z. Zeng, S. Bao, M. Wang, X. Qi, Z. Fan, and H. Zhang, "Solution-phase epitaxial growth of noble metal nanostructures on dispersible single-layer molybdenum disulfide

nanosheets. *Nature communications*, vol.4, no.1, pp1-8.,2013, doi.org/10.1038/ncomms2472
[26] S. Agarwal, and S. Aggarwal, S. "Mucoadhesive polymeric platform for drug delivery; a comprehensive review". *Current drug delivery*, vol.12, no. 2, pp139-156,2015
[27] E. Lee, H. Jeon, M. Lee, J. Ryu, C. Kang, S. Kim, and Y. Kwon, "Molecular origin of AuNPs-induced cytotoxicity and mechanistic study". *Scientific reports*, vol,9, no. 1, pp 1-13,2019, doi.org/10.1038/s41598-019-39579-3
[28] H. Deng, M. Zheng, Z. Hu, X. Zeng, N. Kuang and Y. Fu, "Effects of daphnetin on the autophagy signaling pathway of fibroblast-like synoviocytes in rats with collagen-induced arthritis (CIA) induced by TNF-alpha". *Cytokine*. vol. 127, P 154952, 2019, doi.org/10.1016/j.cyto.2019.154952
[29] J. Jhaveri, Z. Raichura, T. Khan, M. Momin, and A. Omri, A. "Chitosan nanoparticles-insight into properties, functionalization and applications in drug delivery and theranostics". *Molecules*, vol,26, no. 2, p272, 2021, doi.org/10.3390/molecules26020272

[30] A.C. Marques, P.J. Costa, S. Velho, and M.H. Amaral" Functionalizing nanoparticles with cancer-targeting antibodies: A comparison of strategies". *Journal of Controlled Release*, vol. 320, PP 180-200, 2020, doi.org/10.1016/j.jconrel.2020.01.035

[31] S. Gao, F. Rojas-Vega, J. Rocha-Martin, and J.M. Guisán, "Oriented immobilization of antibodies through different surface regions containing amino groups: Selective immobilization through the bottom of the Fc region". *International Journal of Biological Macromolecules*, vol. 177, pp19-28,2021, doi.org/10.1016/j.ijbiomac.2021.02.103

[32] A. Tomak, S. Cesmeli, B.D. Hanoglu, D. Winkler, and C. Oksel Karakus, "Nanoparticle-protein corona complex: understanding multiple interactions between environmental factors, corona formation, and biological activity". *Nanotoxicology*, vol. 15, no. 10, pp1331-1357.,2021, doi.org/10.1080/17435390.2022.2025467
[33] J.D. Lambris, D. Ricklin and B.V. Geisbrecht, "Complement evasion by human pathogens". *Microbiology*, vol. 6, no. 2, p132–142,2008, doi.org/10.1038/nrmicro1824
[34] F. Chen, G. Wang, J.I. Griffin, B. Brenneman, N.K. Banda, V. M. Holers, and D. Simberg, **"Complement** proteins bind to nanoparticle protein corona and undergo dynamic exchange *in vivo*". *Nature nanotechnology*, vol. 12, no. 4, pp387-393,2017, doi.org/10.1038/nnano.2016.269
[35] A. Kondo and J. Mihara, "Comparison of adsorption and conformation of hemoglobin and myoglobin on various inorganic ultrafine particles". *Journal of colloid and interface science*, vol. 177, no. 1, pp214–21,1995
[36] Brown, D. M., Dickson, C., Duncan, P., Al-Attili, F., & Stone, V. (2010). "Interaction between nanoparticles and cytokine proteins: impact on protein and particle functionality". *Nanotechnology*, vol. 21, no. 21, p215104.
[37] L. Lynch A. Salvati and K.A. Dawson, "Protein–nanoparticle interactions: what does the cell see?" *Nature nanotechnology*, vol.4, no. 9, PP546–7,2009, doi.org/10.1038/nnano.2009.248
[38] D.M. Brown V. Stone P. Findlay W. MacNee and K. Donaldson K, "Increased inflammation and intracellular calcium caused by ultrafine carbon black is independent of transition metals or

other soluble components". *Occupational and Environmental Medicine*. Vol. 57, no.10, pp 685–91,2000, dx.doi.org/10.1136/oem.57.10.685

